The non-receptor tyrosine kinase Lyn controls neutrophil adhesion by recruiting the CrkL–C3G complex and activating Rap1 at the leading edge

Yuan He[1], Ashish Kapoor[2], Sara Cook[1], Shubai Liu[3], Yang Xiang[3], Christopher V. Rao[2], Paul J. A. Kenis[2,4] and Fei Wang[1,4,*]

[1]Department of Cell and Developmental Biology, University of Illinois at Urbana-Champaign, Urbana, IL 61801, USA
[2]Department of Chemical and Biomolecular Engineering, University of Illinois at Urbana-Champaign, Urbana, IL 61801, USA
[3]Department of Molecular Integrative Physiology, University of Illinois at Urbana-Champaign, Urbana, IL 61801, USA
[4]Institute for Genomic Biology, University of Illinois at Urbana-Champaign, Urbana, IL 61801, USA
*Author for correspondence (feiwang@life.uiuc.edu)

Accepted 22 February 2011
Journal of Cell Science 124, 2153-2164

doi:10.1242/jcs.078535

Summary

Establishing new adhesions at the extended leading edges of motile cells is essential for stable polarity and persistent motility. Despite recent identification of signaling pathways that mediate polarity and chemotaxis in neutrophils, little is known about molecular mechanisms governing cell–extracellular-matrix (ECM) adhesion in these highly polarized and rapidly migrating cells. Here, we describe a signaling pathway in neutrophils that is essential for localized integrin activation, leading edge attachment and persistent migration during chemotaxis. This pathway depends upon G_i-protein-mediated activation and leading edge recruitment of Lyn, a non-receptor tyrosine kinase belonging to the Src kinase family. We identified the small GTPase Rap1 as a major downstream effector of Lyn to regulate neutrophil adhesion during chemotaxis. Depletion of Lyn in neutrophil-like HL-60 cells prevented chemoattractant-induced Rap1 activation at the leading edge of the cell, whereas ectopic expression of Rap1 largely rescued the defects induced by Lyn depletion. Furthermore, Lyn controls spatial activation of Rap1 by recruiting the CrkL–C3G protein complex to the leading edge. Together, these results provide novel mechanistic insights into the poorly understood signaling network that controls leading edge adhesion during chemotaxis of neutrophils, and possibly other amoeboid cells.

Key words: Lyn, Adhesion, Neutrophil chemotaxis, Rap1, CrkL

Introduction

Cell migration has been conceptualized as a cycle (Ridley et al., 2003). After a stimulus, cells polymerize actin at the front to initiate protrusions. These protrusions are stabilized by adhering to extracellular matrix (ECM) molecules (adhesion). Adhesions serve as traction sites as the cell moves forward, and are disassembled at the rear, allowing the cell to detach and retract. In general, strategies for single-cell migration can be classified into two patterns: amoeboid movement and mesenchymal migration (Friedl, 2004). Slow-moving mesenchymal cells (e.g. fibroblasts) often adopt a spindle-shaped morphology and adhere via large integrin-mediated plaque-like structures called focal adhesions. By contrast, fast-moving cells (e.g. neutrophils) use amoeboid movement associated with fast deformability and highly polarized morphology, and move more rapidly. Unlike the mesenchymal migration paradigm, large focal adhesions seen in slow moving fibroblasts and stress fibers are not detected in these cells (Friedl, 2004), suggesting fundamental differences between amoeboid and mesenchymal cell adhesions; however, integrin-mediated adhesion is necessary for persistent cell migration (Ley et al., 2007).

When exposed to chemoattractants, neutrophils polarize and initiate polymerization of actin at the leading edge (pseudopod) to provide the protrusive force. Primary neutrophils and neutrophil-like cells have complex signaling pathways that control formation of their front and back. A ‘frontness’ pathway containing Rac, the lipid products of phosphoinositide-3-kinases (PI3Ks) and polymerized actin organizes the leading edge of neutrophils, whereas the ‘backness’ signals, including Rho, p160–ROCK and myosin II, lead to contraction of actin–myosin complexes at the trailing edge, causing cells to de-adhere (Srinivasan et al., 2003; Wang et al., 2002; Xu et al., 2003).

Despite these advances, little is known about the regulation of cell–ECM adhesion during chemotaxis. Frontness and backness responses per se do not entirely account for the persistent polarity and motility of neutrophils when they are exposed to chemoattractants. Indeed, chemoattractant stimulation of neutrophils in suspension (i.e. without cell adhesion to the substrate) only causes transient membrane extension, in sharp contrast to cells stimulated on substrates, which polarize and migrate persistently (Srinivasan et al., 2003; Wang et al., 2002; Xu et al., 2003). In circulating neutrophils β2 integrins (CD18) are highly expressed and mediate the interactions of neutrophils with endothelial cells. The importance of β2-integrin-mediated adhesion in neutrophil chemotaxis is highlighted by patients with leukocyte adhesion deficiency (LAD), who have decreased numbers of neutrophils at the sites of infection and inflammation (Bunting et al., 2002). These findings imply a crucial role of cell–substrate adhesion in the regulation of neutrophil polarity and motility.

To dissect the molecular program that governs adhesion of the neutrophil leading edge during chemotaxis, we assessed the role of proteins known to be involved in signaling from chemoattractant receptors and integrins. One such protein is the non-receptor

tyrosine kinase Lyn, which belongs to the Src kinase family. Emerging evidence suggests that Lyn has a role in modulating integrin signaling and cell migration in hematopoietic cells (Baruzzi et al., 2008; Maxwell et al., 2004; O'Laughlin-Bunner et al., 2001). For instance, neutrophil adhesion to fibrinogen leads to activation and redistribution of Lyn to the cytoskeletal fractions (Yan et al., 1996). Furthermore, Lyn can also be activated by several chemoattractants in human neutrophils and is required for the formation of phosphatidylinositol-3,4,5-trisphosphate (Gaudry et al., 1995; Ptasznik et al., 1996). Interestingly, deletion of Lyn in mouse neutrophils leads to enhanced integrin-mediated cell responses (Pereira and Lowell, 2003), suggesting that Lyn has a negative role in integrin signaling events. Despite these findings, how Lyn is involved in the regulation of chemoattractant-stimulated neutrophil migration has not been well defined. Here, we describe a Lyn-dependent mechanism for promoting localized integrin activation and establishing adhesion sites at the leading edge to allow neutrophils to move forward in the chemoattractant gradient.

Results

Lyn expression, activation and localization

To understand how Lyn controls chemotaxis, we determined its expression, activity and subcellular localization in neutrophils. Lyn was highly expressed in primary human neutrophils and the neutrophil-like differentiated HL-60 cells (dHL-60), but not in undifferentiated HL-60 cells or non-hematopoietic HEK293 cells (supplementary material Fig. S1A). The upper and lower bands represent the Lyn A and Lyn B isoform, respectively, as previously reported (Yi et al., 1991). Differentiated HL-60 cells have been used widely for studying neutrophil polarity and chemotaxis (Bodin and Welch, 2005; Gomez-Mouton et al., 2004; Hauert et al., 2002; Nuzzi et al., 2007; Schymeinsky et al., 2006): when differentiated, they exhibit neutrophil morphology, polarize in response to attractants, and migrate in gradients of attractant at rates comparable to primary neutrophils (Servant et al., 2000; Wang et al., 2002; Xu et al., 2003). Unlike primary neutrophils, they can be continuously cultured and are genetically tractable (Neel et al., 2009; Servant et al., 2000; Srinivasan et al., 2003; Weiner et al., 2006; Xu et al., 2003). In this study, we used fibrinogen as the ECM substrate to recapitulate the physiological microenvironment for neutrophil migration. Fibrinogen is a known ligand for β2 integrin in neutrophils (Altieri et al., 1990).

We analyzed the activity of Lyn by immunoprecipitating endogenous Lyn from dHL-60 cell lysates, followed by assessment of the level of activated Lyn using an antibody specific for phosphorylated Src proteins. Phosphorylation of tyrosine residues (at Tyr397 for Lyn) in the activation loop of the kinase domain upregulates enzyme activity of Src kinase family (Hunter, 1987). Exposure of suspended cells (i.e. in the absence of ECM attachment) to the bacteria-derived chemoattractant formyl-Met-Leu-Phe (fMLP) induced rapid and robust activation of Lyn, reaching a maximum at 30 seconds (6.1±2.4-fold above resting condition; mean ± s.e.m.), as detected by the phospho-specific antibody (Fig. 1A). Treatment of cells with pertussis toxin (PTX) completely abolished Lyn activation (Fig. 1B). Covalent modification of the α-subunit of G_i by PTX inactivates G_i and abrogates all frontness signals (Xu et al., 2003). By contrast, inhibition of PI3K with a specific inhibitor, LY294002, prevented fMLP-induced Akt phosphorylation as expected, but failed to affect Lyn activation (Fig. 1B and data not shown). Thus, fMLP-stimulated Lyn activation depends upon G_i but not PI3K.

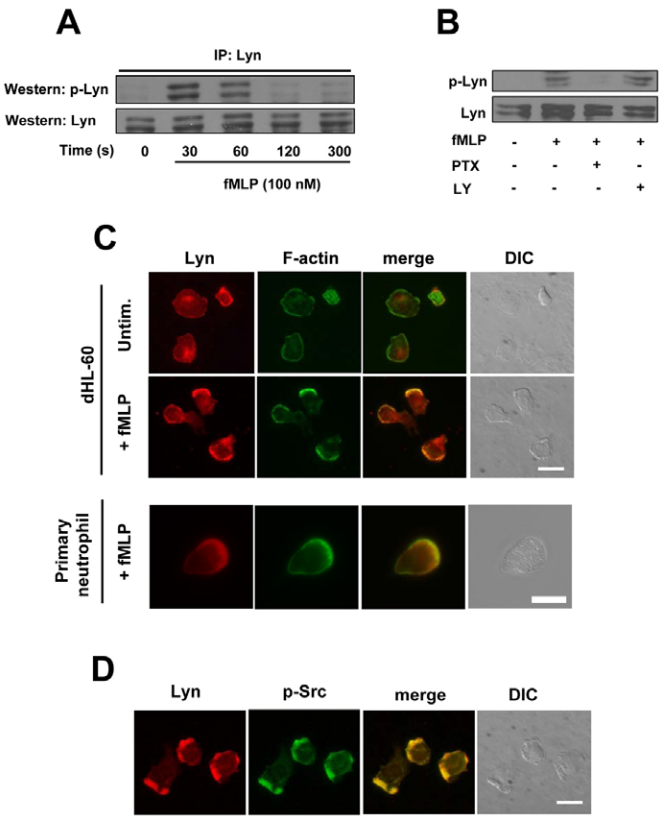

Fig. 1. Lyn activation and localization. (**A**) Phosphorylation of Lyn in response to fMLP stimulation (100 nM) for various time points. (**B**) Western blot analysis of tyrosine-phosphorylated Lyn (p-Lyn) in dHL-60 cells pretreated with buffer, PTX (1 μg/ml, O/N) or LY-294002 (200 μM, 2 hours) and stimulated with fMLP (100 nM, 1 minute). (**C**) Immunofluorescence of Lyn (red) and F-actin (green) in cells plated on fibrinogen without or with fMLP stimulation (100 nM, 2 minutes). Lyn and F-actin merged images and DIC images of cells are also shown. (**D**) Immunofluorescence images of Lyn (red) and phosphorylated Src (green) in cells plated on fibrinogen with a uniform concentration of fMLP (100 nM, 2 minutes). Scale bars: 10 μm.

Interestingly, when exposed to fMLP, cells plated on the fibrinogen substrate exhibited a relatively small increase in phosphorylated Lyn (10–20%), which was sustained for over 10 minutes (data not shown). The distinct patterns of Lyn activation between suspended and adherent cells suggested differential regulation of Lyn activity under these conditions.

Immunofluorescence of Lyn in non-stimulated adherent dHL-60 cells was distributed cortically around the plasma membranes, with some cytoplasmic localization, but was preferentially distributed to the leading edge of 73% of cells (out of 415 examined) treated with fMLP, where it colocalized with F-actin (Fig. 1C). The immunofluorescence was specific for Lyn, as verified by competition experiments with a blocking peptide (supplementary material Fig. S1B). The asymmetry of Lyn in fMLP-treated cells was not caused by increased amounts of membrane at the front, as shown by dual imaging of Lyn and a fluorescent membrane dye (DiD) in the same cells (supplementary material Fig. S1C). Although membranes were uniformly located and in some cases slightly enriched at the leading edge, there was a significant increase in Lyn, as shown by the merged images (supplementary material Fig. S1C). fMLP-induced leading edge recruitment of Lyn was

also seen in primary neutrophils (Fig. 1C, bottom panel). In addition, fMLP also stimulated asymmetrical accumulation of phosphorylated Src (activated Src) proteins, in patterns that were highly reminiscent of total Lyn (Fig. 1D). Immunofluorescence of phosphorylated Src was mostly attributed to phosphorylated Lyn protein, because RNAi-mediated depletion of Lyn (see below) nearly completely abolished the phosphorylated Src immunofluorescence (supplementary material Fig. S1D). Thus, Lyn is activated and translocates to the leading edge in response to fMLP.

Depletion of Lyn impairs neutrophil chemotaxis

We next assessed the effect of Lyn depletion on dHL-60 chemotaxis (Figs 2, 3). We transiently knocked down the expression of genes of interest in dHL-60 cells by using the Amaxa Nucleofection System, allowing us to quickly test genes involved in the regulation of neutrophil chemotaxis. Transfection of cells with a pool of siRNAs targeting human Lyn reduced Lyn protein by ~80% after 48 hours (Fig. 2A,B). In addition, we used a lentivirus-based system to stably express small hairpin RNAs (shRNAs) that efficiently depleted Lyn in dHL-60 cells, enabling us to conduct

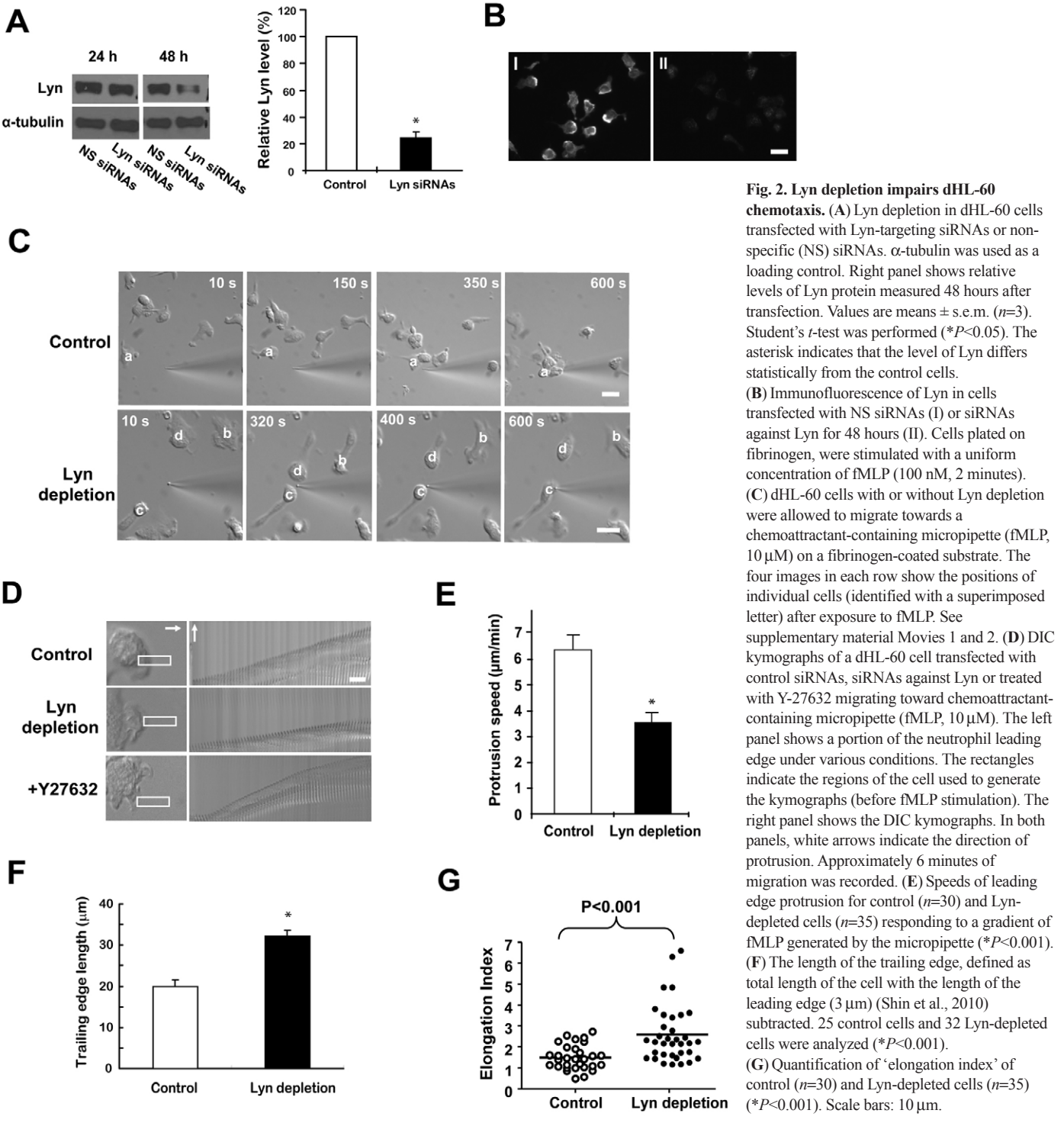

Fig. 2. Lyn depletion impairs dHL-60 chemotaxis. (**A**) Lyn depletion in dHL-60 cells transfected with Lyn-targeting siRNAs or non-specific (NS) siRNAs. α-tubulin was used as a loading control. Right panel shows relative levels of Lyn protein measured 48 hours after transfection. Values are means ± s.e.m. (n=3). Student's t-test was performed (*P<0.05). The asterisk indicates that the level of Lyn differs statistically from the control cells. (**B**) Immunofluorescence of Lyn in cells transfected with NS siRNAs (I) or siRNAs against Lyn for 48 hours (II). Cells plated on fibrinogen, were stimulated with a uniform concentration of fMLP (100 nM, 2 minutes). (**C**) dHL-60 cells with or without Lyn depletion were allowed to migrate towards a chemoattractant-containing micropipette (fMLP, 10 μM) on a fibrinogen-coated substrate. The four images in each row show the positions of individual cells (identified with a superimposed letter) after exposure to fMLP. See supplementary material Movies 1 and 2. (**D**) DIC kymographs of a dHL-60 cell transfected with control siRNAs, siRNAs against Lyn or treated with Y-27632 migrating toward chemoattractant-containing micropipette (fMLP, 10 μM). The left panel shows a portion of the neutrophil leading edge under various conditions. The rectangles indicate the regions of the cell used to generate the kymographs (before fMLP stimulation). The right panel shows the DIC kymographs. In both panels, white arrows indicate the direction of protrusion. Approximately 6 minutes of migration was recorded. (**E**) Speeds of leading edge protrusion for control (n=30) and Lyn-depleted cells (n=35) responding to a gradient of fMLP generated by the micropipette (*P<0.001). (**F**) The length of the trailing edge, defined as total length of the cell with the length of the leading edge (3 μm) (Shin et al., 2010) subtracted. 25 control cells and 32 Lyn-depleted cells were analyzed (*P<0.001). (**G**) Quantification of 'elongation index' of control (n=30) and Lyn-depleted cells (n=35) (*P<0.001). Scale bars: 10 μm.

large-scale biochemical analyses (supplementary material Fig. S1E). When exposed to an external fMLP gradient, delivered by a micropipette, cells transfected with non-specific siRNAs formed well-defined leading and trailing edges and migrated rapidly and persistently towards the tip of the micropipette (Fig. 2C; supplementary material Movie 1). By contrast, although Lyn-depleted cells were capable of responding to the fMLP gradient and establishing a leading edge in the direction of the pipette, they protruded significantly slower than control cells. Kymograph analysis showed that the protrusion speeds for control and Lyn-depleted cells were 6.32±0.44 μm/minute and 3.64±0.31 μm/minute (mean ± s.e.m.), respectively (Fig. 2D,E). Concomitant to decreased protrusion, the speed for trailing edge retraction was also reduced in Lyn-depleted cells (5.03±0.25 μm/minute for control vs 1.61±0.23 μm/minute for Lyn depletion). In addition, the cell bodies of Lyn-depleted cells were unable to detach effectively from the substrate and remained largely stationary, resulting in a stretched spindle-shaped morphology (Fig. 2C; supplementary material Movie 2) and long trailing edges (32.2±1.3 μm vs 19.8±1.6 μm for controls) (Fig. 2F). In keeping with this result, the elongation index (the ratio of the length of a polarized cell when fully extended to the width of its pseudopod) of Lyn-depleted cells was greater than that of control cells (2.63±0.23 vs 1.61±0.11, respectively) (Fig. 2G). At late stages of stimulation (>6 minutes), some of the Lyn-depleted cells (~26%) retracted their leading edges (Fig. 2C; cells b and d).

Interestingly, treatment of dHL-60 cells with PP2, a highly specific inhibitor of Src kinase family, failed to mimic the phenotypes of Lyn depletion. In the micropipette assay, PP2 treatment caused cells to slightly increase the protrusion and migration speeds (data not shown). A similar result was reported: treatment of mouse and human neutrophils with PP2 did not alter

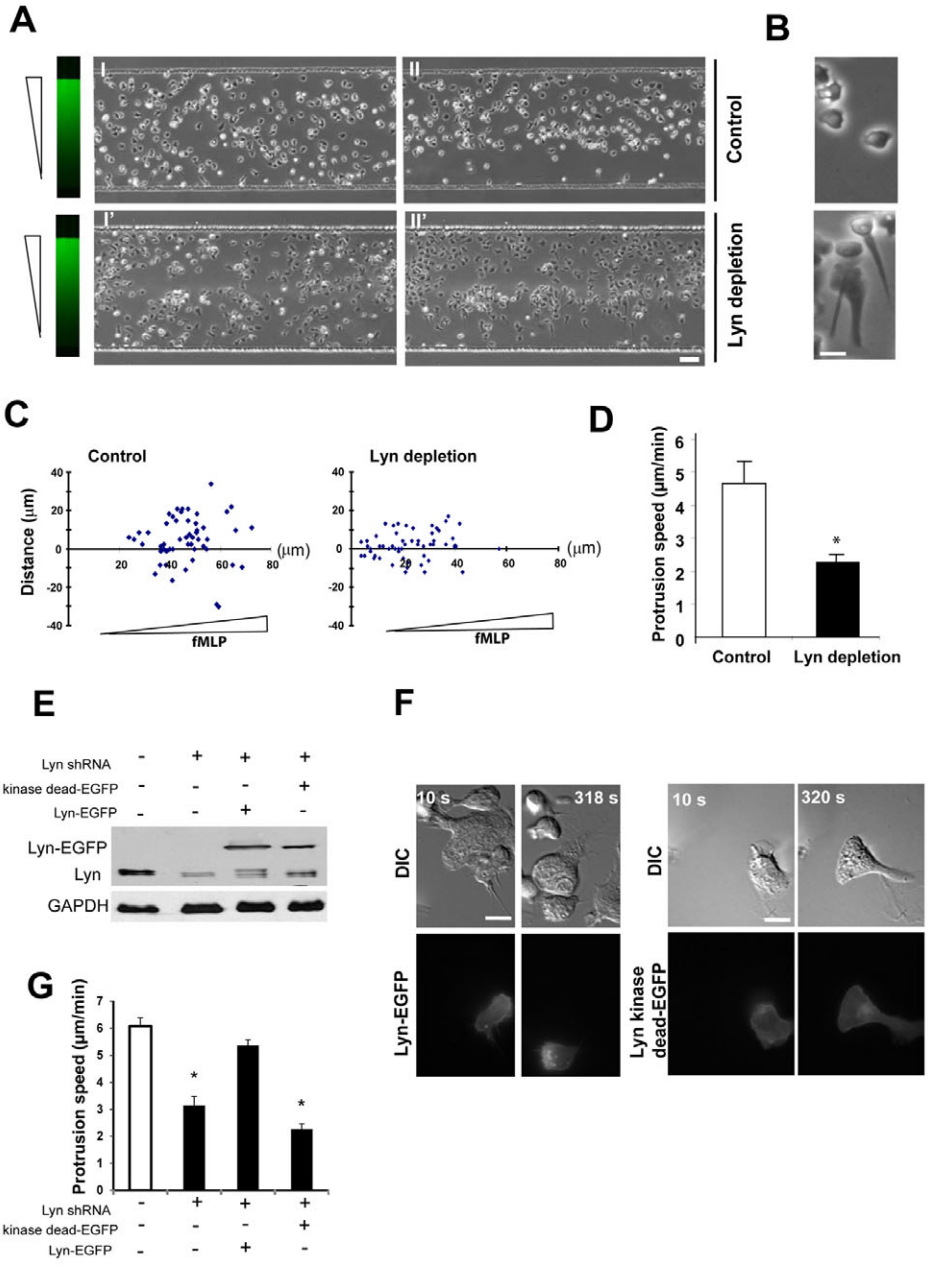

Fig. 3. Lyn depletion impairs dHL-60 chemotaxis in a microfluidic gradient device. (**A**) Phase-contrast images of control (I,II) and Lyn-depleted cells (I′,II′) in the microfluidic chamber coated with the fibrinogen substrate before (I,I′) and after (II,II′) exposure to an fMLP gradient (10 minutes) generated by the microfluidic device. The gradient can be traced by fluorescent dyes such as fluorescein (left). Scale bar: 50 μm. Movies of cells with or without Lyn depletion are available as supplementary material Movies 3, 4. (**B**) Enlarged views of control cells (top) and Lyn-depleted cells (bottom) 10 minutes after the stimulation of the fMLP gradient. Scale bar: 10 μm. (**C**) The positions of control and Lyn-depleted cells at the end of the experiments were plotted, in relation to their starting position at the origin. *X*-axis shows the distance along the fMLP gradient. *Y*-axis shows the distance vertical to the fMLP gradient. (**D**) Speeds of leading edge protrusion for control and Lyn-depleted cells responding to a gradient of fMLP generated by the microfluidic device. The values are means ± s.e.m. (n=47 for control, n=46 for Lyn-depleted cells) (*P<0.001). (**E**) Western blotting of Lyn in control and Lyn-depleted cells with or without rescue. Lyn-depleted cells were differentiated and transfected with GFP-tagged wild-type Lyn56 or kinase-dead dominant-negative mutant of Lyn56 (K275D) containing silent mutations in the shRNA-targeting region. GAPDH is the loading control. (**F**) GFP-tagged wild-type Lyn, but not kinase-dead (K275D) Lyn mutant, rescues the defects of Lyn-depleted cells. Time-lapse images of representative cells for both conditions are shown. Scale bar: 10 μm. (**G**) Speeds of leading edge protrusion for control, Lyn-depleted, Lyn-rescued cells revealed with the micropipette assay. Values are means ± s.e.m. (n=12 for control, n=15 for Lyn shRNA alone, n=11 for Lyn shRNA plus Lyn-EGFP and n=13 for Lyn shRNA plus Lyn kinase-dead–EGFP). Asterisks indicate that the cells differ statistically from the control cells (*P<0.001).

neutrophil migration in experiments with the Transwell assay (Fumagalli et al., 2007). The differential effects between Lyn depletion and PP2 treatment might be due to potential complex interplay between members of the Src kinase family. Expression of a number of Src family kinases was documented in neutrophils (Korade-Mirnics and Corey, 2000; Lowell, 2004).

The chemotactic behavior of Lyn-depleted cells was also examined with a microfluidic gradient device, which assesses migration of cell populations in highly stable gradients over a long distance (Fig. 3). Time-lapse videomicroscopy could track individual cells as they migrated in the microfluidic chamber (Fig. 3A). In this assay, Lyn depletion markedly impaired neutrophil chemotaxis in an fMLP gradient (1.4 nM/μm) (supplementary material Fig. S1F). In contrast to untreated cells (Fig. 3A,B, top panel; Fig. 3D; supplementary material Movie 3), Lyn-depleted cells protruded more slowly and exhibited an elongated morphology (Fig. 3A,B, bottom panel; Fig. 3D; supplementary material Movie 4). These defects were similar to those seen in the micropipette assay. Notably, the chemotactic index [the ratio of migration in the correct direction to the actual length of the migration path (Xu et al., 2005)] was similar between control and Lyn-depleted cells (0.93 and 0.91, respectively), suggesting that Lyn depletion did not impair directionality of the cells (Fig. 3C).

The chemotactic defects in Lyn-depleted cells were probably caused by the lack of Lyn kinase activity, Expression of a GFP-tagged dominant-negative kinase-dead Lyn mutant (LynK275D) in dHL-60 cells led to defects similar to those seen with Lyn depletion (supplementary material Fig. S1G). Furthermore, transfection of wild-type Lyn, but not the kinase-dead mutant, largely rescued the defects of Lyn depletion (Fig. 3E,F,G). Together, these results suggest that Lyn kinase activity might be responsible for Lyn-mediated functions in neutrophils during chemotaxis.

Lyn is not required for the 'frontness' signals

We next assessed the mechanism by which Lyn controls neutrophil chemotaxis. The asymmetrical localization of Lyn and the effect of Lyn depletion on cell protrusion led us to investigate a potential role in establishment of the leading edge. It was reported previously that actin polymers, phospatidylinositol-3,4,5-trisphosphate (PIP3) and Rac-GTP are key components of the 'frontness' pathway that controls leading edge establishment during neutrophil chemotaxis (Srinivasan et al., 2003; Xu et al., 2003). We therefore assessed whether Lyn depletion reduced these signals. We took advantage of a unique feature of neutrophils: their ability to polarize when stimulated with chemoattractants, even in suspension. When exposed to fMLP, neutrophils in suspension quickly (within 1–2 minutes) establish a morphological leading edge (Zhelev et al., 2004). The leading edge does not persist, and retracts after stimulation (Fechheimer and Zigmond, 1983; Sklar et al., 1985; Wang et al., 2002; Ydrenius et al., 1997). Attractant stimulation of suspended neutrophils also suffices to accumulate polymerized actin, PIP3 and Rac-GTP, albeit transiently, consistent with the morphological response (Srinivasan et al., 2003; Wang et al., 2002; Xu et al., 2003). This feature of neutrophils enables us to assess the frontness response without input introduced by the outside-in signals from cell–ECM adhesion. Under these conditions Lyn depletion failed to prevent the accumulation of polymerized actin, Rac-GTP and phosphorylated Akt (activated Akt, readout for PIP3) in neutrophils exposed to fMLP stimulation (supplementary material Fig. S2A–C), suggesting that signaling pathways leading to PI3K, Rac and F-actin activation or formation are not altered by Lyn depletion.

Lyn is required for localized activation of β2 integrin and leading edge adhesion

During migration, protrusion and adhesion of the leading edge are coupled (Ridley et al., 2003). Therefore, the defects of Lyn depletion on neutrophil chemotaxis could be due to inability of these cells to attach their protrusive pseudopods, resulting in slower protrusion. This notion is supported by the observation that at late stages of fMLP stimulation, some Lyn-depleted neutrophils detached and retracted their leading edges, implying that the cells failed to stably adhere to the ECM substrate at the front. Thus, Lyn might regulate leading edge adhesion, leading us to assess whether Lyn controls β2 integrin in neutrophils. In control cells, β2 integrin immunofluorescence was mostly distributed at the leading edge after fMLP stimulation, with some diffused localization in the cell body. The asymmetrical distribution of β2 integrin was confirmed quantitatively by using the ratio of immunofluorescence intensity of β2 integrin between the leading edge and the cell body (2.54±0.31; mean ± s.e.m.) (Fig. 4A,C). The use of the ratio of mean fluorescence intensity discounts variations in the levels of fluorescence among cells and is thus more appropriate for assessing relative accumulation of the fluorescent signals. Lyn depletion did not change the asymmetry of β2 integrin localization (2.64±0.19) (Fig. 4A,C). By contrast, although activated β2 integrin, assessed by using antibody m24, exhibited a similar leading edge enrichment in control cells (Ratio: 2.52±0.27), Lyn depletion markedly impaired this enrichment (1.35±0.03) (Fig. 4B,C).

To investigate whether attenuated β2 integrin activity might be responsible for the defects of Lyn depletion, we assessed the effect of a β2 integrin function-blocking antibody (IB4) on neutrophil migration. We plated dHL-60 cells on fibrinogen and then treated them with different doses of IB4 for a short period (10 minutes) before fMLP stimulation. This procedure selectively prevented fMLP-induced de novo adhesion without significantly altering global adhesion of cells to the fibrinogen substrates (see Materials and Methods). In the presence of non-specific IgG, dHL-60 cells migrated towards the source of fMLP and maintained a highly polarized morphology with well-developed pseudopods (Fig. 4D, top panel). By contrast, cells treated with the intermediate dose of IB4 (0.1 μg/ml) migrated with slower protruding leading edges [3.12±0.24 μm/minute vs 5.84±0.38 μm/minute for IgG-treated cells (n=33 cells for each condition)] and exhibited elongated morphologies (Fig. 4D, middle panel). Furthermore, at a higher dose (0.5 μg/ml), IB4 treatment caused some cells (~28%) to only transiently polarize in response to fMLP, with much smaller leading edges and a rounded-up morphology, which was probably due to stronger inhibition of leading edge adhesion (Fig. 4D, bottom panel). Thus, blocking cell adhesion with an intermediate dose of IB4 mirrored Lyn depletion (Fig. 2C).

It was reported previously that deletion of Lyn causes mouse neutrophils to become hyper-adhesive when they are adherent to surfaces coated with ECM proteins (Pereira and Lowell, 2003). Similarly, Lyn-depleted dHL-60 cells exhibited increased adhesion to fibrinogen in the absence of fMLP (supplementary material Fig. S3A). However, in contrast to control cells, which markedly elevated adhesion after fMLP stimulation, Lyn-depleted cells only showed a moderate increase (supplementary material Fig. S3A). There was no difference in surface expression of β2 integrin between control and Lyn-depleted cells (supplementary material Fig. S3B), which is consistent with results in mouse neutrophils (Pereira and Lowell, 2003). To determine whether elevated adhesion was responsible for the chemotactic defects of Lyn-

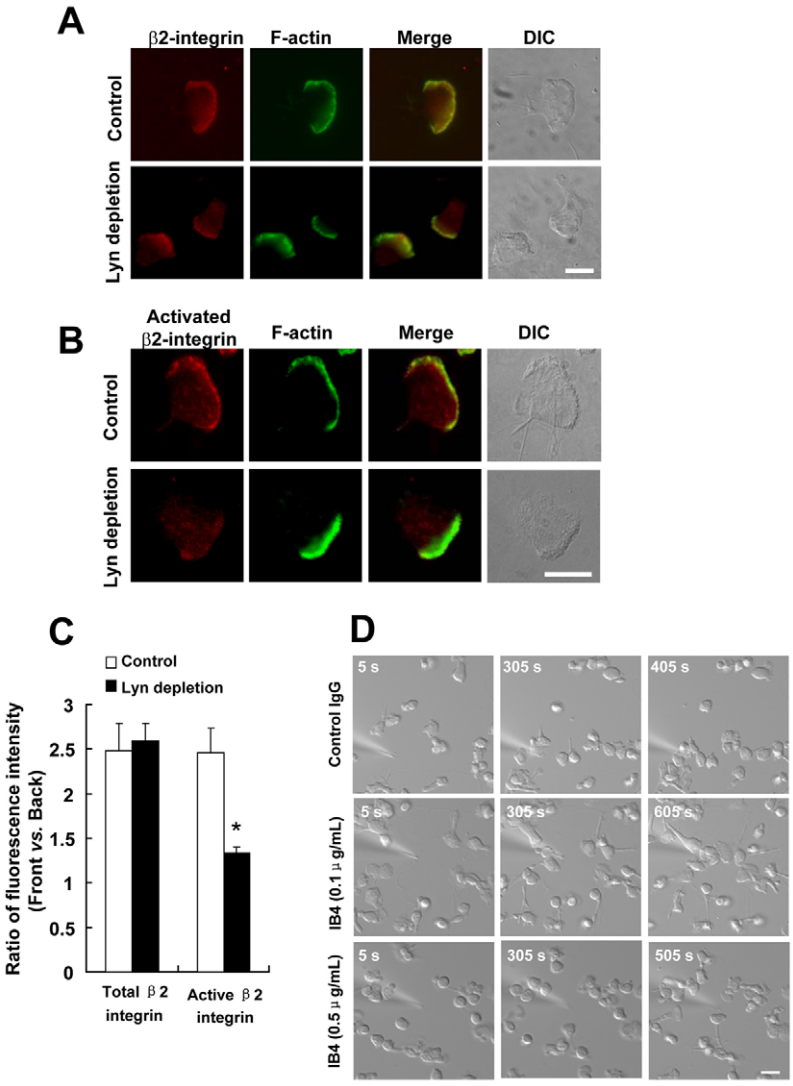

Fig. 4. Lyn depletion attenuates β2 integrin activation at the leading edge. (**A**) Immunofluorescence of β2 integrin (red) in cells with or without Lyn depletion, stimulated with a uniform concentration of fMLP (100 nM, 2 minutes). Fluorescent images of F-actin (green), F-actin and β2 integrin merged images and DIC images of cells are also shown. Scale bar: 10 μm. (**B**) Immunofluorescence of active β2 integrin (red), stained with antibody m24, in cells with or without Lyn depletion, stimulated with a uniform concentration of fMLP (100 nM, 2 minutes). Fluorescent images of F-actin (green), F-actin and active β2 integrin merged images, and DIC images of cells are also shown. Scale bar: 10 μm. (**C**) Front versus back ratio of fluorescence intensity in A and B. The region containing actin staining is defined as front, whereas the rest of the cell is defined as back. Fluorescence intensity in the regions of front and back was quantified by ImageJ. The ratios for control cells (37 cells for total β2-integrin and 45 cells for active β2 integrin) and Lyn-depleted cells (53 cells for total β2 integrin and 46 for active β2 integrin) were calculated. (**D**) Blocking front de novo adhesion mimics the defects of Lyn depletion in chemotaxis. Time-lapse images from three representative experiments are shown.

depleted cells, we treated cells with Mn^{2+}, which triggers β2 integrin activation (Altieri, 1991), causing neutrophils to tightly adhere to the fibrinogen substrate and fail to polarize morphologically in response to an fMLP gradient (supplementary material Fig. S3C). Immunofluorescence studies showed that although the level of activated β2 integrin was high after Mn^{2+} treatment, F-actin was largely diffusely distributed (supplementary material Fig. S3D).

Notably, the defects of Lyn depletion are reminiscent of those induced by inhibiting the backness signals, which caused neutrophils to form highly stretched long tails (Xu et al., 2003). However, we showed that Lyn was not involved in the regulation of the backness pathway or myosin-II-mediated contractions (supplementary material Fig. S3E–G). Lyn depletion failed to alter RhoA activity or the level of activated myosin II (phosphorylated specifically at Ser19) (supplementary material Fig. S3E–G). By contrast, treatment of cells with the p160-ROCK inhibitor Y-26732 markedly reduced the level of phosphorylated myosin II. Furthermore, in contrast to Lyn depletion, treatment with Y-27632, which prevented trailing edge retraction, did not alter the speed for leading edge protrusion (5.91±0.37 μm/minute) (Fig. 2D). This result is consistent with earlier findings (Shin et al., 2010), again demonstrating differential effects between Lyn depletion and inhibition of the backness signals.

Rap1 is a major effector of Lyn in neutrophils during chemotaxis

The Ras-like small GTPase Rap1 has emerged as a major mediator of inside-out signaling to integrins (Bos, 2005; Caron et al., 2000; Shimonaka et al., 2003). Rap1 controls chemokine-induced integrin activation and adhesion (Shimonaka et al., 2003), leading us to assess whether Rap1 acted as a downstream target of Lyn in neutrophils during chemotaxis.

We assayed Rap1–GTP (the activated form of Rap1) by using a previously described pull-down method (Zwartkruis et al., 1998). Rap1–GTP levels increased transiently in suspended dHL-60 cells after exposure to fMLP, reaching a maximum at 30 seconds (>10-fold above unstimulated control; Fig. 5A). fMLP stimulation also caused adherent cells to markedly increase the levels of Rap1–GTP, which sustained after stimulation (supplementary material Fig. S4A,B and data not shown). A similar activation pattern was reported in primary neutrophils (M'Rabet et al., 1998). Rap1 activation was also observed in live cells responding to a gradient of fMLP, which induced GFP–RalGDS translocation from the cytosol to plasma

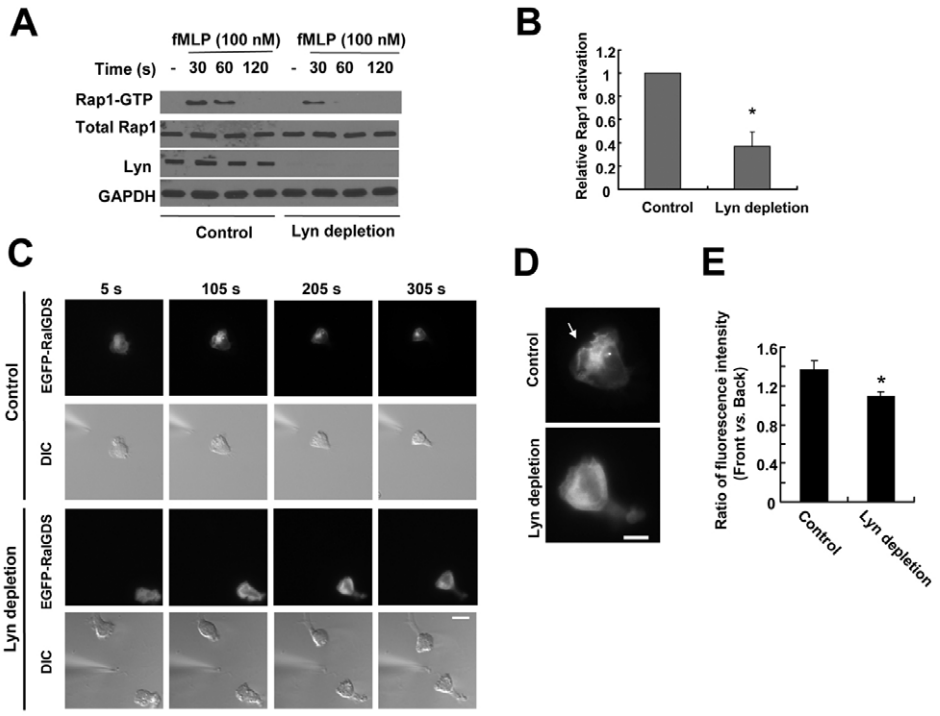

Fig. 5. Lyn is required for Rap1 activation and translocation to the leading edge. (**A**) The levels of Rap1–GTP in dHL-60 cells under various conditions. dHL-60 cells with or without Lyn depletion were stimulated with 100 nM of fMLP for various time points and lysed for the pull-down assay. Levels of total Rap1 and GAPDH were used to show cell lysate input. The blot for Lyn is also shown. (**B**) Quantification of relative levels of Rap1–GTP level in dHL-60 cells with and without Lyn depletion 30 seconds after fMP stimulation. Each bar represents the mean ± s.e.m. (error bars). Values are normalized to the level of Rap1–GTP (=1) in cells without Lyn depletion (**P*<0.001). (**C**) dHL-60 cells with or without Lyn depletion were transfected with EGFP–RalGDS and stimulated by an fMLP-containing micropipette for indicated times. EGFP–RalGDS fluorescence and the corresponding DIC images are shown. (**D**) Enlarged views of EGFP–RalGDS-expressing cells with or without Lyn depletion after stimulation with fMLP. The arrow indicates leading edge recruitment of EGFP–RalGDS. (**E**) Ratios of mean fluorescence intensity of EGFP–RalGDS between the front and the back of cells. The front of the cell is defined as the area within the first 4 μm of the cell, whereas the rest of the cell was defined as the back (**P*<0.01).

membranes at the ruffling leading edge (Fig. 5C,D, top panel). GFP–RalGDS is a fluorescent probe for Rap1–GTP (Wang et al., 2006). A quantitative analysis of the fluorescence intensity across the cells revealed a steep gradient of GFP signals in untreated control cells (78±21% decrease) (supplementary material Fig. S4C). By contrast, GFP-tagged Rap1 was largely uniformly distributed in the cytoplasm in unstimulated cells and remained diffusely distributed after fMLP stimulation (Fig. 6D), suggesting that the asymmetrical accumulation was specific for activated Rap1.

Lyn depletion markedly inhibited fMLP-induced activation of Rap1. We found that Lyn depletion reduced fMLP-induced Rap1 activation by 63±12% in suspended cells (at 30 seconds) (Fig. 5A,B) and 41±9% in adherent cells (supplementary material Fig. S4A,B). Interestingly, in adherent cells without fMLP stimulation, Lyn depletion increased the level of activated Rap1, in keeping with increased cell adhesion and suggesting that Lyn might inhibit Rap1 activity under this condition (supplementary material Fig. S4A,B). In addition, Lyn-depleted cells exhibited poor leading edge recruitment of GFP–RalGDS, as reflected by much more diffuse localization and smaller GFP gradients across the cell (36±15% decrease) (Fig. 5C,D, bottom panel; supplementary material Fig. S4C). Moreover, when compared with control cells, the ratio of mean fluorescence intensity of GFP–RalGDS between the leading edge and the trailing edge was markedly reduced by Lyn depletion (1.40±0.25 for control vs 1.17±0.11 for Lyn depletion, respectively), again revealing that asymmetrical localization of activated Rap1 was impaired (Fig. 5E). Thus, Lyn is required for chemoattractant-induced activation and asymmetrical accumulation of Rap1–GTP at the neutrophil leading edge.

In addition, Rap1 depletion induced chemotactic defects that were highly reminiscent of those caused by Lyn depletion. Two shRNA constructs effectively reduced the level of Rap1A (Fig. 6A), the predominant isoform of Rap1 in neutrophils (Quilliam et al., 1991). In accordance with previous reports (Duchniewicz et al., 2006; Li et al., 2007), Rap1 depletion decreased the number of adherent dHL-60 cells plated on fibrinogen-coated substrate (supplementary material Fig. S4D). When stimulated with a point source of fMLP, Rap1A-depleted cells protruded much more slowly than cells containing non-targeting shRNA (3.43±0.35 μm/minute for Rap1A shRNA1 and 2.96±0.13 μm/minute for Rap1A shRNA2, vs 5.85±0.20 μm/minute for non-targeting shRNA). Furthermore, similarly to Lyn-depleted cells, Rap1A-depleted cells retracted significantly slower (0.83±0.12 μm/minute vs 4.66±0.45 μm/minute for control cells) and developed a spindle-shaped morphology (Fig. 6B,C; supplementary material Movie 5). The elongation index for Rap1A-depleted cells was 2.5±0.32 (*n*=23), which is close to the value for Lyn-depleted cells.

Together, these results suggested that Rap1 acts as a major downstream effector of Lyn in neutrophils during chemotaxis. This inference was further confirmed by effects of overexpression of GFP–Rap1A in Lyn-depleted cells. Ectopic expression of Rap1 nearly completely rescued the defects caused by Lyn depletion (Fig. 6D). In cells overexpressing GFP–Rap1, the average speed for leading edge protrusion was increased to 5.83±0.48 μm/minute, and the elongation index was reduced to 1.74±0.21 μm/minute (*n*=15), even when Lyn was nearly entirely depleted. These values approached those of the control cells without Lyn depletion.

Lyn recruits the CrkL–C3G complex to the leading edge

Previous studies demonstrated that the Crk family adaptors function downstream of activated receptor tyrosine kinases, bind and regulate C3G, a guanine nucleotide exchange factor (GEF) for Rap1, and consequently control Rap1 activation (Arai et al., 1999; Sattler and Salgia, 1998). We found that human primary neutrophils and dHL-60 cells express in high abundance Crk-like protein (CrkL), a member of the Crk family. Interestingly, Crk-I, which is expressed in many cell types, was nearly undetectable (supplementary material Fig. S4E). We thus focused on CrkL and

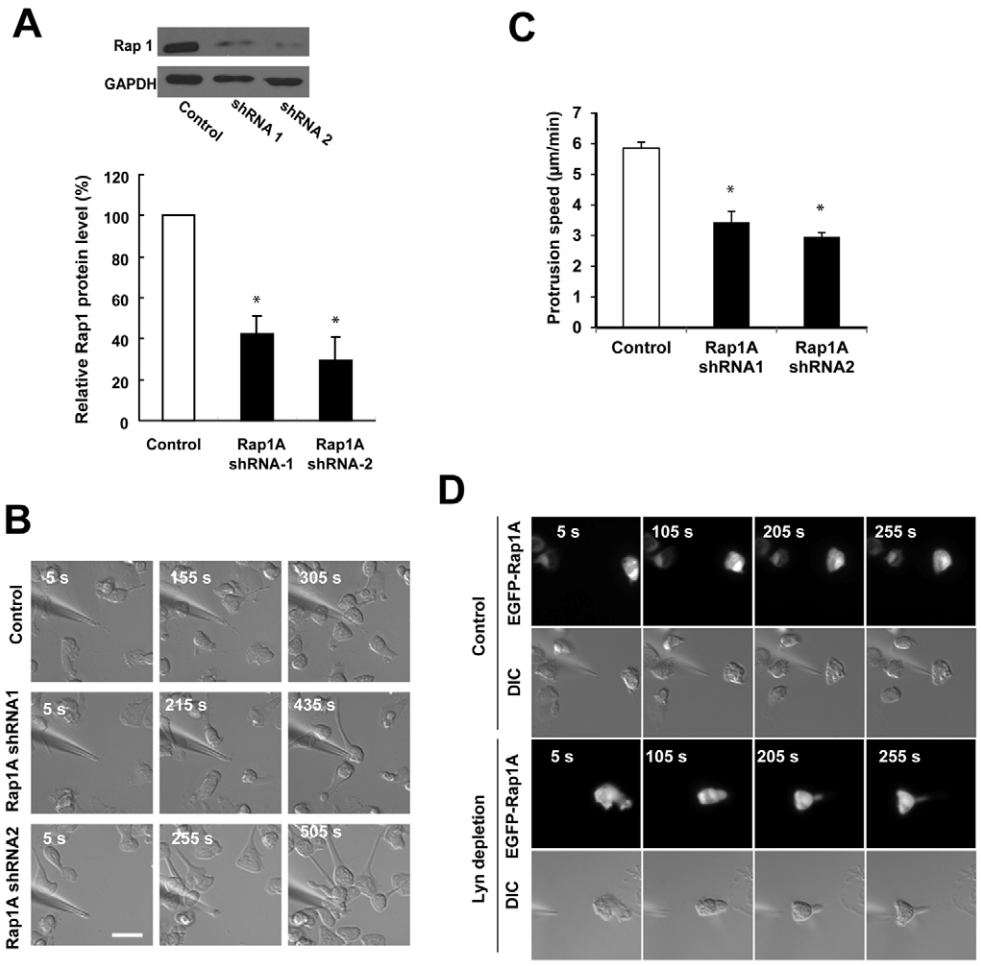

Fig. 6. Rap1A depletion mimics the chemotactic defects of Lyn depletion. (**A**) Western blotting of Rap1A in dHL-60 cells with or without shRNAs targeting Rap1A. GAPDH is a loading control. Bottom panel shows relative level of Rap1 protein is measured in cells containing non-targeting shRNAs (Control) or two Rap1A-targeting shRNAs. Values are means ± s.e.m. (n=3). The asterisks indicate that the level of Rap1 differ statistically from the control cells (*P<0.05). (**B**) dHL-60 cells with Rap1A depletion (Rap1A shRNAs) or without (Control, with non-targeting shRNAs) stimulated on a fibrinogen-coated substrate by a point source of fMLP. The four images in each row show the positions of individual cells after exposure to fMLP. Movies are available in supplementary material as supplementary material Movie 5. (**C**) Speeds of leading edge protrusion for control and Rap1A-depleted cells in the micropipette assay. The values are means ± s.e.m. (n=36 cells for each condition). Asterisks indicate that Rap1A-depleted cells differ statistically from the control cells (*P<0.001). (**D**) dHL-60 cells with or without Lyn depletion were transfected with EGFP–Rap1A and stimulated with a fMLP-containing micropipette. Scale bar: 10 μm.

asked whether it was involved in the regulation of Rap1 by Lyn. The tyrosine residue Y207, located in the small region between two SH3 domains of CrkL, is crucial for the regulation of CrkL activity: phosphorylation of Y207 promotes intramolecular association of CrkL, leading to inhibition (de Jong et al., 1997; Rosen et al., 1995; Senechal et al., 1998). Using a specific antibody, we found that level of phosphorylation at Y207 (Y207-*P*) remained largely unaltered in control cells after fMLP stimulation (Fig. 7A). By contrast, the level of Y207-*P* was significantly higher in Lyn-depleted cells with and without fMLP stimulation (1.5-2.3-fold above control cells; Fig. 7A). Thus, Lyn modulates the removal of the phosphate group from Y207, thereby relieving CrkL inhibition in neutrophils.

Lyn is also involved in the regulation of the subcellular localization of CrkL. Immunofluorescence of CrkL was distributed diffusely in the cytosol and in the cortical areas of the control neutrophils in the absence of fMLP and translocated and accumulated at the leading edge, where it colocalized with F-actin (Fig. 7B and data not shown). C3G exhibited a very similar pattern (Fig. 7C). By contrast, depletion of Lyn impaired leading edge recruitment of CrkL and C3G (Fig. 7B,C). Both proteins were located more diffusively throughout the cell bodies, even though the cells were morphologically polarized. The ratios of mean fluorescence intensity between the leading edge and the trailing edge were reduced from 3.41±0.15 to 1.6±0.34 for CrkL and from 2.64±0.13 to 1.14±0.09 for C3G, respectively.

Consistently with earlier reports, we found that CrkL co-immunoprecipitated with C3G in neutrophils (supplementary material Fig. S4F). This interaction was detected in resting dHL-60 cells and was unaltered after fMLP stimulation. Furthermore, the interaction between CrkL and C3G was also detected in Lyn-depleted cells. Thus, Lyn appears unnecessary for the formation or the stability of the CrkL–C3G protein complex, but is instead essential for its spatial organization.

CrkL is required for Rap1 activation and neutrophil chemotaxis

We next asked whether CrkL acted upstream of Rap1 in neutrophils during chemotaxis. We found that CrkL depletion in dHL-60 cells caused Rap1 activity in fMLP-stimulated cells to reduce by 41% (Fig. 7D). CrkL depletion also caused severe chemotactic defects (Fig. 7E,F). First, CrkL-depleted cells protruded significantly slower (3.01±0.18 μm/minute for CrkL shRNA1 and 2.57±0.29 μm/minute for CrkL shRNA2, vs 6.03±0.36 μm/minute for cells containing non-targeting shRNAs). Furthermore, 68% (17 of 25 cells examined) developed a stretched elongated morphology when responding a point source of fMLP, which was highly reminiscent of the defects of Lyn- and Rap1-depleted cells. In addition, 20% of CrkL-depleted cells failed to develop a stable leading edge, similarly to cells challenged with high concentrations of IB4 (Fig. 4D, bottom panel). Together, these results indicate that Rap1 is a major effector of CrkL in neutrophils during chemotaxis.

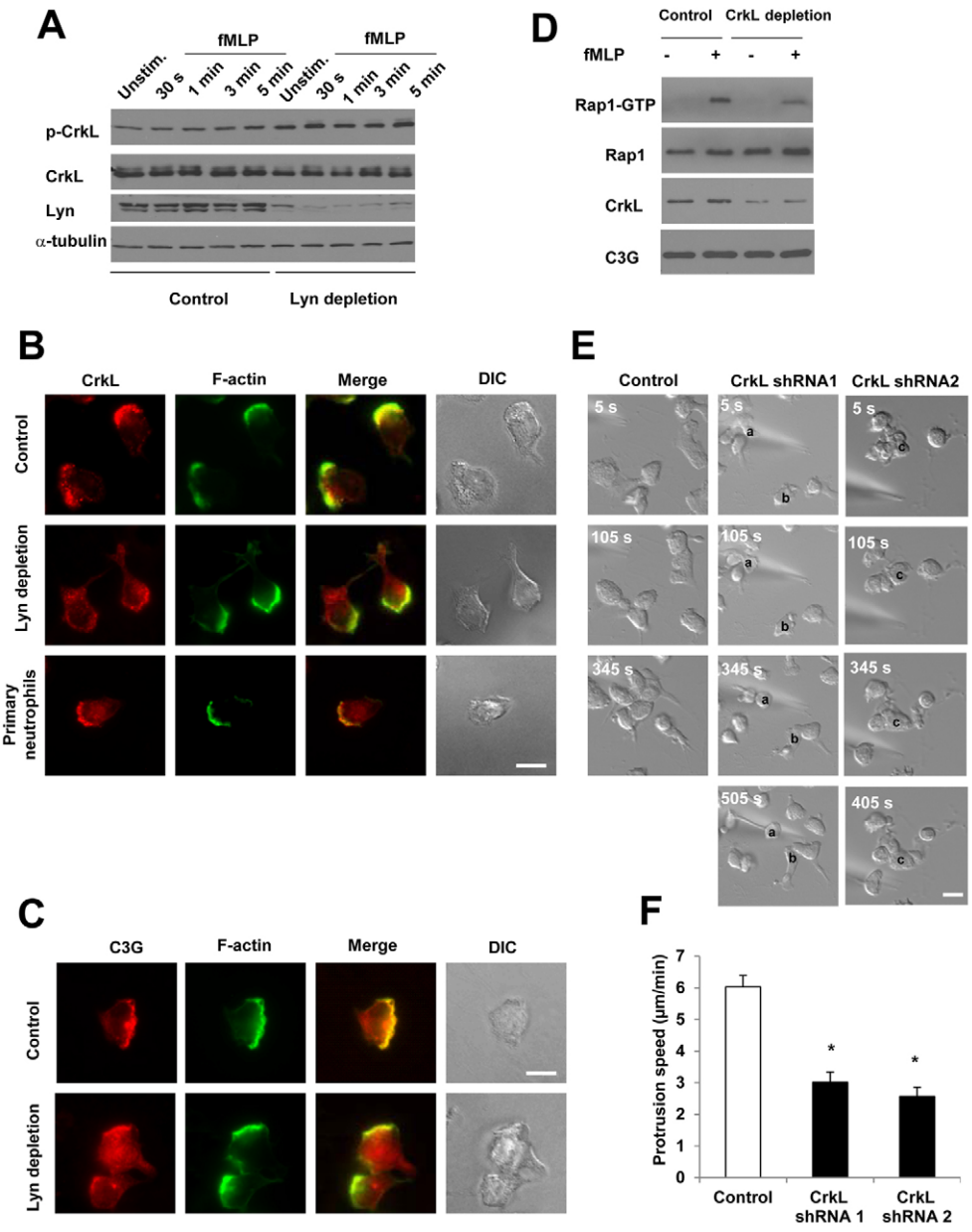

Fig. 7. Lyn is required for the functions of CrkL–C3G complex in neutrophils. (**A**) Western blotting of phosphorylated CrkL (p-CrkL, at Y207) in dHL-60 cells with or without Lyn depletion. Cells were unstimulated or stimulated in suspension with 100 nM fMLP for various times. CrkL and α-tubulin were loading controls. Lyn expression was also analyzed. (**B**,**C**) Immunofluorescence of CrkL and C3G in dHL-60 cells with or without Lyn depletion. Cells were stimulated with a uniform concentration of fMLP (100 nM, 2 minutes). Immunofluorescence of CrkL in human primary neutrophils is also shown. (**D**) Levels of Rap1–GTP in dHL-60 cells with or without CrkL depletion 30 seconds after fMLP stimulation. 30 seconds of fMLP stimulation gave rise to maximal Rap1 activation (Fig. 5A). Blot for total Rap1 shows input from cell lysates for each condition. Blots for CrkL and C3G are also shown. (**E**) dHL-60 cells with or without CrkL depletion were stimulated with a micropipette containing fMLP. The images in each row show the positions of individual cells (identified with a superimposed letter) after exposure to fMLP. Scale bars: 10 μm. (**F**) Speeds of leading edge protrusion for control and CrkL-depleted cells assessed with the micropipette assay. Values are means ± s.e.m. (n=35 for control, n=25 for CrkL shRNA1, n=29 for CrkL shRNA2). Asterisks indicate that CrkL-depleted cells differ statistically from the control cells (*P<0.001).

Discussion

Cell migration is a tightly regulated process that requires adhesion of the extended leading edge to the ECM substrate to ensure uninterrupted migration. Although the understanding of cell adhesion in slow-migrating mesenchymal cells has been significantly improved in the past two decades, this key step remains poorly defined in highly polarized and rapidly moving amoeboid cells, including neutrophils. Recent studies with human neutrophils led to the discovery of signaling pathways that are essential for the establishment of the neutrophil protrusive leading edge. However, there are significant gaps in our understanding of the mechanisms that govern integrin-mediated leading edge adhesion during chemotaxis. In this study, we identified a signaling mechanism that controls localized integrin activation and leading edge adhesion during neutrophil chemotaxis. A model is proposed based on these findings, whereby a central regulatory role is assigned to the non-receptor tyrosine kinase Lyn (Fig. 8). In this scenario, G_i-dependent Lyn activation and translocation to the leading edge is necessary for the relief of inhibition and spatial organization of the CrkL–C3G complex at the leading edge, which leads to localized activation of the small GTPase Rap1 and its downstream target, β2 integrin. Together, these results provide novel mechanistic insights into a crucial but poorly studied facet of neutrophil chemotaxis – adhesion of the protrusive leading edge.

We demonstrated a crucial role for Lyn in regulating leading edge adhesion in chemotaxing neutrophils. First, in response to chemoattractants, Lyn is activated and recruited to leading edge of polarized neutrophils. Depletion of Lyn impairs leading edge protrusion but fails to prevent chemoattractant-induced activation of Rac, polymerized actin or PI3Ks, suggesting that Lyn regulates leading edge adhesion, not initial establishment of the leading edge. Second, although some Lyn-depleted cells exhibited a morphological defect that was similar to that of

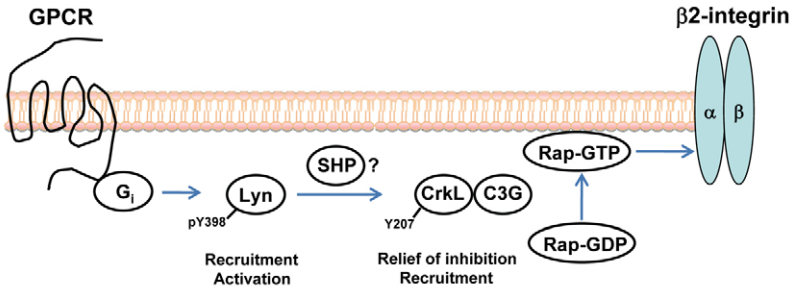

Fig. 8. A biochemical pathway required for leading edge adhesion, localized β2 integrin activation and persistent migration in neutrophils during chemotaxis: a model. G_i-dependent Lyn activation and translocation to the leading edge is necessary for the relief of inhibition and spatial organization of the CrkL–C3G complex at the leading edge, which leads to localized activation of the small GTPase Rap1 and β2 integrin. GPCR, G-protein-coupled receptor.

cells with an impaired backness pathway, Lyn depletion did not impair the activity of this pathway. Indeed, a fraction of Lyn-depleted cells retracted their leading edges when exposed to fMLP, a defect rarely seen in cells with the backness pathway inhibited. Moreover, treatment of cells with Y-27632, unlike Lyn depletion, failed to impair leading edge protrusion. At the mechanistic level, Lyn depletion impaired localized activation of β2 integrin, which appears to be responsible for the chemotactic defects induced by Lyn depletion, because inhibition of de novo leading edge adhesion with intermediate concentration of IB4 mimicked the phenotype of Lyn depletion. In addition, we identified Rap1, a well-recognized regulator of β2 integrin activity, as a major downstream effector of Lyn in neutrophils during chemotaxis.

How might partial inhibition of leading edge adhesion (e.g. with Lyn or Rap1 depletion, or the treatment with intermediate dose of IB4) lead to an elongated cellular morphology in neutrophils? We speculate that this defect might result from the inability of the cells to establish firm adhesion sites at the front, a prerequisite for translocation of the cell body and de-attachment of the trailing edge. Indeed, in each condition wherein leading edge adhesion is impaired, there is a concomitant reduction in retraction speeds, suggesting linkage between front adhesion and tail retraction. Furthermore, inhibition of the backness pathway per se (e.g. with Y-27632) did not affect protrusion, again implying that compromised retraction in Lyn- and Rap1A-depleted cells, as well as in cells treated with intermediated dose of IB4, might originate from defects in leading edge adhesion. More complete understanding of the detailed mechanisms underlying the morphological defects awaits future experiments.

In comparison to earlier studies, our findings provide a more detailed and comprehensive delineation of the function of Lyn in neutrophils during chemotaxis. In keeping with earlier studies in Lyn-deficient mouse neutrophils (Pereira and Lowell, 2003), our data show that without fMLP stimulation, Lyn-depleted cells exhibit enhanced adhesion to the fibrinogen substrate and exhibit higher Rap1 activity, suggesting that Lyn might inhibit Rap1 activity under this condition. By contrast, in the presence of fMLP, Lyn depletion markedly reduced Rap1 activity and consequently impairs local activation of β2 integrin in dHL-60 cells. Furthermore, addition of Mn^{2+}, which induces β2 integrin activation, caused neutrophils to tightly adhere to the fibrinogen substrate and fail to polarize in response to a chemoattractant gradient – a phenotype that is distinct from that of Lyn-depleted cells. Together, these results suggest differential regulation and wiring of the chemotactic signaling network in cells with and without attractant stimulation. In agreement with this notion, Gakidis and co-workers (Gakidis et al., 2004) showed that Vav1, Vav2 and Vav3 (GEFs for Rac and Cdc42), are required for the integrin-dependent functions of mouse neutrophils, including sustained adhesion, spreading and complement-mediated phagocytosis, but are dispensable for fMLP-induced signaling events and chemotaxis, even when cells are assessed on the same ECM substrate (Gakidis et al., 2004). Together, these results highlight the complexity of chemotactic signaling networks that control neutrophil chemotaxis and underscore the importance of studying cell–ECM interactions as an integral part of the global chemotactic response. Notably, we did not observe an increase in total β2 integrin activity in Lyn-depleted dHL-60 cells after fMLP stimulation in suspension (Y.H. and F.W., unpublished observations), in contrast to a previous study in Lyn-inhibited hematopoietic cells stimulated with SDF-1α (Nakata et al., 2006). The differential effects of Lyn depletion or inhibition might be attributed to differences in cell type and chemoattractant. Alternatively, it might be that the experiments for the detection of active β2 integrin were conducted in suspended cells with prolonged incubation with the m24 β2 integrin antibody and fMLP, which did not recapitulate the chemotaxis conditions and might also contribute to the variation.

Our results suggest that the CrkL–C3G protein complex acts as a key signaling intermediate that controls Lyn-dependent spatial activation of Rap1 in neutrophils. In this scenario, CrkL associates constitutively with the Rap1 GEF C3G, as in hematopoietic cells and other cell types. Upon exposure to chemoattractant, the CrkL–C3G complex is recruited to the leading edge of polarized neutrophils, providing spatially instructive cues for localized Rap1 activation (Fig. 8). Lyn mediates the leading edge recruitment of CrkL–C3G, but probably not by direct physical interactions: we did not detect Lyn protein in CrkL or C3G immunoprecipitates (Y.H. and F.W., unpublished observations). Instead, we speculate that other Lyn-interacting proteins, such as hematopoietic cell-specific Lyn substrate 1 (HS1) (Uruno et al., 2003) or the Shc adaptor protein (Ptasznik et al., 1995) might have a special role in mediating the recruitment. In addition, we have shown that Lyn modulates CrkL function by the removal of Y207 phosphorylation, thereby relieving the intramolecular inhibition of CrkL. It is of note that the kinetics of Y207 phosphorylation differs from Lyn activation: in response to fMLP, the level of Y207-*P* remains largely unaltered, whereas Lyn activity is markedly elevated. Therefore, it is not clear whether Lyn expression, or its activity, modulates CrkL Y207 dephosphorylation. We postulate that the tyrosine phosphatase SH-2 domain phosphatase (SHP), reportedly a downstream target of Lyn (Pereira and Lowell, 2003) (Fig. 8), might be responsible for the removal of Y207 phosphorylation. However, although SHP-1 was recruited to the leading edge of neutrophils, the attempt to produce SHP-1-depleted dHL-60 cells failed in our experiments (Y.H. and F.W., unpublished observations).

Materials and Methods

Reagents and plasmids

Human fibrinogen, human serum albumin (HSA) and fMLP were from Sigma. Y-27632, LY 294002 and pertussis toxin were from Calbiochem. Alexa Fluor 488 phalloidin and Alexa Fluor 647 phalloidin were from Invitrogen. ON-TARGETplus SMARTpool siRNAs, which contain four siRNAs specifically targeting human Lyn, non-specific siRNAs and siGLO were from Dharmacon. All antibodies for western and/or immunofluorescence analyses are listed in supplementary material Table S1.

The DNA sequences for Lyn 53/56 were amplified from dHL-60 cell genomic DNA using PCR and cloned into pcDNA3 with the gene encoding EGFP at the C-terminus. The dominant-negative mutant of Lyn 56 (K275D) (Corey et al., 1998) and both shRNA-resistant mutants of wild-type Lyn 56 and Lyn 56(K275D) were generated by site-directed mutagenesis. Mammalian expression vector encoding pEGFP-C3/Rap1A and pcDNA3-EGFP-RalGDS were provided by Mark Philips (New York University, New York, NY) (Bivona et al., 2004) and Philip Stork (The Vollum Institute, Portland, OR) (Wang et al., 2006), respectively. shRNAs targeting Lyn, Rap1A and CrkL are described in supplementary material Table S2.

Cell culture, transient transfection, lentiviral production and infection

Cultivation and differentiation of HL-60 cells were described previously (Wang et al., 2002). Transient transfections of dHL-60 cells was as described (Shin et al., 2010). For lentiviral production, shRNA-containing plasmids were cotransfected with three packaging plasmids pPL1, pPL2 and pPL/VSVG (Invitrogen) into actively growing HEK293T cells. After 3 days of transfection, supernatant containing lentiviral particles was concentrated using Lenti-X concentrator (Clontech) and added to growing HL-60 cells in the presence of 10 μg/ml polybrene for 24 hours. Lyn-knockdown cells were enriched by cell sorting (Cytomation Plus, Dako) (for pSicoR constructs) or selected in the presence of 0.5 μg/ml puromycin for 2 weeks (for PLKO.1 constructs).

Immunofluorescence and live-cell imaging

Immunofluorescence analysis and the detection of F-actin of in dHL-60 cells and human neutrophils were as described (Shin et al., 2010), except that cells were plated on human fibrinogen-coated cover glasses (250 μg/ml) (Schymeinsky et al., 2005).

For live-cell imaging, cells were plated on fibrinogen-coated surface for 20 minutes, washed briefly, and subsequently stimulated either with a uniform concentration of 100 nM fMLP or a point source of 10 μM fMLP from a micropipette as described (Servant et al., 2000). To analyze the effects of inhibiting de novo cell adhesion on chemotaxis, dHL-60 cells were plated on fibrinogen-coated surface for 20 minutes and washed briefly. Adherent cells were then incubated with different concentrations of IB4 antibody (0.1 μg/ml or 0.5 μg/ml) or with mouse isotype IgG for 10 minutes before stimulation with the fMLP-containing micropipette. DIC images, fluorescent images and combined DIC/fluorescence images were collected with a Zeiss 40× NA 1.30 Fluar DIC objective or 63× NA 1.4 Plan Apochromat DIC objective on a Zeiss Axiovert 200M microscope. All images were collected with a cooled charge-coupled device camera (AxioCam MR3, Zeiss) and processed using the ImageJ program. Kymograph analysis of leading edge protrusion was conducted as described previously (Shin et al., 2010).

Immunoprecipitation and western blotting

Cells (5×10^6) were suspended in mHBSS buffer and stimulated with 100 nMfMLP for indicated time points. fMLP stimulation was terminated by the addition of RIPA buffer (1×, 50 mM Tris-HCl, pH 7.5, 1% NP-40, 150 mM NaCl, 1 mM EDTA) containing 1 mM Na_3VO_4, 1 mM NaF, 1 mM PMSF and a protease inhibitor cocktail (Sigma). After clarification, cell lysates were pre-cleared with protein A beads and thereafter incubated with 2 μg of anti-Lyn polyclonal antibody. After 2 hours of incubation at 4°C, protein A beads were added to the cell lysates. The resulting immunoprecipitates were washed with ice-cold RIPA buffer and analyzed further with SDS-PAGE. The procedures for western blotting were described previously (Shin et al., 2010).

Microfluidic gradient device

The microfluidic gradient device comprises of a polydimethylsiloxane (PDMS) slab embedded with a Y-shaped fluidic channel and glass substrate as its base. The microchannels were fabricated using rapid prototyping and soft lithography as described previously (Herzmark et al., 2007; Jeon et al., 2000; Lin and Butcher, 2006). Cells suspended in mHBSS containing 1% HSA were injected in the microfluidic device and allowed to attach to the fibrinogen substrate (20 minutes). The channels were then gently rinsed with mHBSS to wash away floating cells. To generate soluble gradients, fMLP (500 nM) and mHBSS were infused into the device from separate inlets. Solutions were driven using a syringe infusion pump (Pump 22, Harvard Apparatus) at a flow rate of 0.03 ml/hour to generate a concentration gradient in the channel by diffusion. Images were captured using the Axiovision software (Zeiss).

Rac-GTP and RhoA-GTP assay

An absorbance-based (490 nm) Rac G-LISA kit or RhoA G-LISA (Cytoskeleton) was used to determine Rac–GTP or RhoA–GTP levels in dHL-60. Cells with or without Lyn depletion were suspended in mHBSS (5×10^6 cells) and stimulated or unstimulated with 100 nM fMLP. The reaction was stopped by adding 2× lysis buffer (provided with the kit) at 4°C. Subsequent steps were performed as described in the protocol supplied.

Cell adhesion assay

96-well plates were coated with 100 μg/ml fibrinogen at 4°C O/N and blocked with 2 mg/ml heat-denatured BSA for 1 hour at 37°C. Plates were washed with PBS once before seeding cells into wells. Cells were labeled with calcium AM (5 μM) for 30 minutes, washed and suspended in mHBSS. 4×10^5 cells (100 μl) were loaded into each well. After incubation for 30 minutes with buffer or fMLP (100 nM), each well was washed four times with pre-warmed mHBSS. The remaining cells were then lysed with 100 μl PBS containing 0.1% Triton X-100. The fluorescence intensity of each well was recorded with a microplate reader (SpectraMax M2). The percentage of adherent cells was calculated as the ratio of remaining fluorescence intensity and input fluorescence intensity.

Actin polymerization assay

The procedure for measuring polymerized actin was conducted as described previously (Weiner et al., 2006).

Rap1–GTP assay

A Rap1–GTP Pull-Down and Detection kit (Thermo Scientific) was used. For suspension conditions, dHL-60 cells were suspended in mHBSS (10×10^6 cells for one condition) and stimulated (or unstimulated) with 100 nM fMLP. The reaction was stopped by the addition of 0.4 ml ice-old 1.25× lysis buffer (25 mM Tris-HCl, pH 7.5, 150 mM NaCl, 5 mM $MgCl_2$, 1% NP-40 and 5% glycerol). For adhesion conditions, dHL-60 cells were plated on fibrinogen-coated six-well plates for 20 minutes, stimulated or not stimulated with 100 nM fMLP for 5 minutes, and lysed in 0.5 ml lysis buffer. Subsequent steps were performed according to the manufacturer's instructions.

Isolation of primary neutrophils

Primary neutrophils were isolated from venous blood from healthy human donors using PMN isolation kit (Matrix). Neutrophils were suspended in RPMI 1640 medium supplemented with 10% fetal bovine serum at 37°C until the time of experiments.

We thank Nancy Hogg for providing the m24 monoclonal antibody, Philip Stork for providing the GFP-RalGDS construct, Mark Philips for providing the GFP-Rap1A construct and the members of the Wang lab for helpful discussion. This work was supported by NIH grants GM083812 (to F.W.), GM083601 (to C.V.R. and F.W.), HD059002 (to Deborah Leckband and F.W.), NSF CAREER award 0953267 (to F.W.) and NSF-EBICS award. Deposited in PMC for release after 12 months.

Supplementary material available online at
http://jcs.biologists.org/cgi/content/full/124/13/2153/DC1

References

Altieri, D. C. (1991). Occupancy of CD11b/CD18 (Mac-1) divalent ion binding site(s) induces leukocyte adhesion. *J. Immunol.* **147**, 1891-1898.

Altieri, D. C., Agbanyo, F. R., Plescia, J., Ginsberg, M. H., Edgington, T. S. and Plow, E. F. (1990). A unique recognition site mediates the interaction of fibrinogen with the leukocyte integrin Mac-1 (CD11b/CD18). *J. Biol. Chem.* **265**, 12119-12122.

Arai, A., Nosaka, Y., Kohsaka, H., Miyasaka, N. and Miura, O. (1999). CrkL activates integrin-mediated hematopoietic cell adhesion through the guanine nucleotide exchange factor C3G. *Blood* **93**, 3713-3722.

Baruzzi, A., Caveggion, E. and Berton, G. (2008). Regulation of phagocyte migration and recruitment by Src-family kinases. *Cell. Mol. Life Sci.* **65**, 2175-2190.

Bivona, T. G., Wiener, H. H., Ahearn, I. M., Silletti, J., Chiu, V. K. and Philips, M. R. (2004). Rap1 up-regulation and activation on plasma membrane regulates T cell adhesion. *J. Cell Biol.* **164**, 461-470.

Bodin, S. and Welch, M. D. (2005). Plasma membrane organization is essential for balancing competing pseudopod- and uropod-promoting signals during neutrophil polarization and migration. *Mol. Biol. Cell* **16**, 5773-5783.

Bos, J. L. (2005). Linking Rap to cell adhesion. *Curr. Opin. Cell Biol.* **17**, 123-128.

Bunting, M., Harris, E. S., McIntyre, T. M., Prescott, S. M. and Zimmerman, G. A. (2002). Leukocyte adhesion deficiency syndromes: adhesion and tethering defects involving beta 2 integrins and selectin ligands. *Curr. Opin. Hematol.* **9**, 30-35.

Caron, E., Self, A. J. and Hall, A. (2000). The GTPase Rap1 controls functional activation of macrophage integrin alphaMbeta2 by LPS and other inflammatory mediators. *Curr. Biol.* **10**, 974-978.

Corey, S. J., Dombrosky-Ferlan, P. M., Zuo, S., Krohn, E., Donnenberg, A. D., Zorich, P., Romero, G., Takata, M. and Kurosaki, T. (1998). Requirement of Src kinase Lyn for induction of DNA synthesis by granulocyte colony-stimulating factor. *J. Biol. Chem.* **273**, 3230-3235.

de Jong, R., ten Hoeve, J., Heisterkamp, N. and Groffen, J. (1997). Tyrosine 207 in CRKL is the BCR/ABL phosphorylation site. *Oncogene* **14**, 507-513.

Duchniewicz, M., Zemojtel, T., Kolanczyk, M., Grossmann, S., Scheele, J. S. and Zwartkruis, F. J. (2006). Rap1A-deficient T and B cells show impaired integrin-mediated cell adhesion. *Mol. Cell. Biol.* **26**, 643-653.

Fechheimer, M. and Zigmond, S. H. (1983). Changes in cytoskeletal proteins of polymorphonuclear leukocytes induced by chemotactic peptides. *Cell Motil.* **3**, 349-361.

Friedl, P. (2004). Prespecification and plasticity: shifting mechanisms of cell migration. *Curr. Opin. Cell Biol.* **16**, 14-23.

Fumagalli, L., Zhang, H., Baruzzi, A., Lowell, C. A. and Berton, G. (2007). The Src family kinases Hck and Fgr regulate neutrophil responses to N-formyl-methionyl-leucyl-phenylalanine. *J. Immunol.* **178**, 3874-3885.

Gakidis, M. A., Cullere, X., Olson, T., Wilsbacher, J. L., Zhang, B., Moores, S. L., Ley, K., Swat, W., Mayadas, T. and Brugge, J. S. (2004). Vav GEFs are required for beta2 integrin-dependent functions of neutrophils. *J. Cell Biol.* **166**, 273-282.

Gaudry, M., Gilbert, C., Barabe, F., Poubelle, P. E. and Naccache, P. H. (1995). Activation of Lyn is a common element of the stimulation of human neutrophils by soluble and particulate agonists. *Blood* **86**, 3567-3574.

Gomez-Mouton, C., Lacalle, R. A., Mira, E., Jimenez-Baranda, S., Barber, D. F., Carrera, A. C., Martinez, A. C. and Manes, S. (2004). Dynamic redistribution of raft domains as an organizing platform for signaling during cell chemotaxis. *J. Cell Biol.* **164**, 759-768.

Hauert, A. B., Martinelli, S., Marone, C. and Niggli, V. (2002). Differentiated HL-60 cells are a valid model system for the analysis of human neutrophil migration and chemotaxis. *Int. J. Biochem. Cell Biol.* **34**, 838-854.

Herzmark, P., Campbell, K., Wang, F., Wong, K., El-Samad, H., Groisman, A. and Bourne, H. R. (2007). Bound attractant at the leading vs. the trailing edge determines chemotactic prowess. *Proc. Natl. Acad. Sci. USA* **104**, 13349-13354.

Hunter, T. (1987). A tail of two src's: mutatis mutandis. *Cell* **49**, 1-4.

Jeon, N. J., Dertinger, S. K. W., Chiu, D. T., Choi, I. S., Stroock, A. D. and Whitesides, G. M. (2000). Generation of solution and surface gradients using microfluidic systems. *Langmuir* **16**, 8311-8316.

Korade-Mirnics, Z. and Corey, S. J. (2000). Src kinase-mediated signaling in leukocytes. *J. Leukoc. Biol.* **68**, 603-613.

Ley, K., Laudanna, C., Cybulsky, M. I. and Nourshargh, S. (2007). Getting to the site of inflammation: the leukocyte adhesion cascade updated. *Nat. Rev. Immunol.* **7**, 678-689.

Li, Y., Yan, J., De, P., Chang, H. C., Yamauchi, A., Christopherson, K. W., 2nd, Paranavitana, N. C., Peng, X., Kim, C., Munugalavadla, V. et al. (2007). Rap1a null mice have altered myeloid cell functions suggesting distinct roles for the closely related Rap1a and 1b proteins. *J. Immunol.* **179**, 8322-8331.

Lin, F. and Butcher, E. C. (2006). T cell chemotaxis in a simple microfluidic device. *Lab Chip* **6**, 1462-1469.

Lowell, C. A. (2004). Src-family kinases: rheostats of immune cell signaling. *Mol. Immunol.* **41**, 631-643.

M'Rabet, L., Coffer, P., Zwartkruis, F., Franke, B., Segal, A. W., Koenderman, L. and Bos, J. L. (1998). Activation of the small GTPase rap1 in human neutrophils. *Blood* **92**, 2133-2140.

Maxwell, M. J., Yuan, Y., Anderson, K. E., Hibbs, M. L., Salem, H. H. and Jackson, S. P. (2004). SHIP1 and Lyn Kinase Negatively Regulate Integrin alpha IIb beta 3 signaling in platelets. *J. Biol. Chem.* **279**, 32196-32204.

Nakata, Y., Tomkowicz, B., Gewirtz, A. M. and Ptasznik, A. (2006). Integrin inhibition through Lyn-dependent cross talk from CXCR4 chemokine receptors in normal human CD34+ marrow cells. *Blood* **107**, 4234-4239.

Neel, N. F., Barzik, M., Raman, D., Sobolik-Delmaire, T., Sai, J., Ham, A. J., Mernaugh, R. L., Gertler, F. B. and Richmond, A. (2009). VASP is a CXCR2-interacting protein that regulates CXCR2-mediated polarization and chemotaxis. *J. Cell Sci.* **122**, 1882-1894.

Nuzzi, P. A., Senetar, M. A. and Huttenlocher, A. (2007). Asymmetric localization of calpain 2 during neutrophil chemotaxis. *Mol. Biol. Cell* **18**, 795-805.

O'Laughlin-Bunner, B., Radosevic, N., Taylor, M. L., Shivakrupa DeBerry, C., Metcalfe, D. D., Zhou, M., Lowell, C. and Linnekin, D. (2001). Lyn is required for normal stem cell factor-induced proliferation and chemotaxis of primary hematopoietic cells. *Blood* **98**, 343-350.

Pereira, S. and Lowell, C. (2003). The Lyn tyrosine kinase negatively regulates neutrophil integrin signaling. *J. Immunol.* **171**, 1319-1327.

Ptasznik, A., Traynor-Kaplan, A. and Bokoch, G. M. (1995). G protein-coupled chemoattractant receptors regulate Lyn tyrosine kinase.Shc adapter protein signaling complexes. *J. Biol. Chem.* **270**, 19969-19973.

Ptasznik, A., Prossnitz, E. R., Yoshikawa, D., Smrcka, A., Traynor-Kaplan, A. E. and Bokoch, G. M. (1996). A tyrosine kinase signaling pathway accounts for the majority of phosphatidylinositol 3,4,5-trisphosphate formation in chemoattractant-stimulated human neutrophils. *J. Biol. Chem.* **271**, 25204-25207.

Quilliam, L. A., Mueller, H., Bohl, B. P., Prossnitz, V., Sklar, L. A., Der, C. J. and Bokoch, G. M. (1991). Rap1A is a substrate for cyclic AMP-dependent protein kinase in human neutrophils. *J. Immunol.* **147**, 1628-1635.

Ridley, A. J., Schwartz, M. A., Burridge, K., Firtel, R. A., Ginsberg, M. H., Borisy, G., Parsons, J. T. and Horwitz, A. R. (2003). Cell migration: integrating signals from front to back. *Science* **302**, 1704-1709.

Rosen, M. K., Yamazaki, T., Gish, G. D., Kay, C. M., Pawson, T. and Kay, L. E. (1995). Direct demonstration of an intramolecular SH2-phosphotyrosine interaction in the Crk protein. *Nature* **374**, 477-479.

Sattler, M. and Salgia, R. (1998). Role of the adapter protein CRKL in signal transduction of normal hematopoietic and BCR/ABL-transformed cells. *Leukemia* **12**, 637-644.

Schymeinsky, J., Then, C. and Walzog, B. (2005). The non-receptor tyrosine kinase Syk regulates lamellipodium formation and site-directed migration of human leukocytes. *J. Cell. Physiol.* **204**, 614-622.

Schymeinsky, J., Sindrilaru, A., Frommhold, D., Sperandio, M., Gerstl, R., Then, C., Mocsai, A., Scharffetter-Kochanek, K. and Walzog, B. (2006). The Vav binding site of the non-receptor tyrosine kinase Syk at Tyr 348 is critical for {beta}2 integrin (CD11/CD18)-mediated neutrophil migration. *Blood* **108**, 3919-3927.

Senechal, K., Heaney, C., Druker, B. and Sawyers, C. L. (1998). Structural requirements for function of the Crkl adapter protein in fibroblasts and hematopoietic cells. *Mol. Cell. Biol.* **18**, 5082-5090.

Servant, G., Weiner, O. D., Herzmark, P., Balla, T., Sedat, J. W. and Bourne, H. R. (2000). Polarization of chemoattractant receptor signaling during neutrophil chemotaxis. *Science* **287**, 1037-1040.

Shimonaka, M., Katagiri, K., Nakayama, T., Fujita, N., Tsuruo, T., Yoshie, O. and Kinashi, T. (2003). Rap1 translates chemokine signals to integrin activation, cell polarization, and motility across vascular endothelium under flow. *J. Cell Biol.* **161**, 417-427.

Shin, M. E., He, Y., Li, D., Na, S., Chowdhury, F., Poh, Y. C., Collin, O., Su, P., de Lanerolle, P., Schwartz, M. A. et al. (2010). Spatiotemporal organization, regulation, and functions of tractions during neutrophil chemotaxis. *Blood* **116**, 3297-3310.

Sklar, L. A., Omann, G. M. and Painter, R. G. (1985). Relationship of actin polymerization and depolymerization to light scattering in human neutrophils: dependence on receptor occupancy and intracellular Ca++. *J. Cell Biol.* **101**, 1161-1166.

Srinivasan, S., Wang, F., Glavas, S., Ott, A., Hofmann, F., Aktories, K., Kalman, D. and Bourne, H. R. (2003). Rac and Cdc42 play distinct roles in regulating PI(3,4,5)P3 and polarity during neutrophil chemotaxis. *J. Cell Biol.* **160**, 375-385.

Uruno, T., Zhang, P., Liu, J., Hao, J. J. and Zhan, X. (2003). Haematopoietic lineage cell-specific protein 1 (HS1) promotes actin-related protein (Arp) 2/3 complex-mediated actin polymerization. *Biochem. J.* **371**, 485-493.

Wang, F., Herzmark, P., Weiner, O. D., Srinivasan, S., Servant, G. and Bourne, H. R. (2002). Lipid products of PI(3)Ks maintain persistent cell polarity and directed motility in neutrophils. *Nat. Cell Biol.* **4**, 513-518.

Wang, Z., Dillon, T. J., Pokala, V., Mishra, S., Labudda, K., Hunter, B. and Stork, P. J. (2006). Rap1-mediated activation of extracellular signal-regulated kinases by cyclic AMP is dependent on the mode of Rap1 activation. *Mol. Cell. Biol.* **26**, 2130-2145.

Weiner, O. D., Rentel, M. C., Ott, A., Brown, G. E., Jedrychowski, M., Yaffe, M. B., Gygi, S. P., Cantley, L. C., Bourne, H. R. and Kirschner, M. W. (2006). Hem-1 complexes are essential for Rac activation, actin polymerization, and myosin regulation during neutrophil chemotaxis. *PLoS Biol.* **4**, e38.

Xu, J., Wang, F., Van Keymeulen, A., Herzmark, P., Straight, A., Kelly, K., Takuwa, Y., Sugimoto, N., Mitchison, T. and Bourne, H. R. (2003). Divergent signals and cytoskeletal assemblies regulate self-organizing polarity in neutrophils. *Cell* **114**, 201-214.

Xu, J., Wang, F., Van Keymeulen, A., Rentel, M. and Bourne, H. R. (2005). Neutrophil microtubules suppress polarity and enhance directional migration. *Proc. Natl. Acad. Sci. USA* **102**, 6884-6889.

Yan, S. R., Fumagalli, L. and Berton, G. (1996). Activation of SRC family kinases in human neutrophils. Evidence that p58C-FGR and p53/56LYN redistributed to a Triton X-100-insoluble cytoskeletal fraction, also enriched in the caveolar protein caveolin, display an enhanced kinase activity. *FEBS Lett.* **380**, 198-203.

Ydrenius, L., Molony, L., Ng-Sikorski, J. and Andersson, T. (1997). Dual action of cAMP-dependent protein kinase on granulocyte movement. *Biochem. Biophys. Res. Commun.* **235**, 445-450.

Yi, T. L., Bolen, J. B. and Ihle, J. N. (1991). Hematopoietic cells express two forms of lyn kinase differing by 21 amino acids in the amino terminus. *Mol. Cell. Biol.* **11**, 2391-2398.

Zhelev, D. V., Alteraifi, A. M. and Chodniewicz, D. (2004). Controlled pseudopod extension of human neutrophils stimulated with different chemoattractants. *Biophys. J.* **87**, 688-695.

Zwartkruis, F. J., Wolthuis, R. M., Nabben, N. M., Franke, B. and Bos, J. L. (1998). Extracellular signal-regulated activation of Rap1 fails to interfere in Ras effector signalling. *EMBO J.* **17**, 5905-5912.